Journal of Applied Mechanics and Technical Physics, Vol. 49, No. 3, pp. 417–424, 2008

INTERACTION OF A GAS–DROPLET TURBULENT JET WITH A COCURRENT HIGH-VELOCITY HIGH-TEMPERATURE GAS FLOW

D. V. Sadin, A. N. Dobrolyubov, V. P. Zyuzlikov, K. V. Mogilenko, and B. E. Sinil'shchikov

UDC 532.517+536.24

A mathematical model and a method for calculating a gas–droplet turbulent jet with allowance for velocity nonequilibrium and virtual mass of the condensed phase during turbulent fluctuations and also heat and mass transfer within the three-temperature scheme are developed. Methodical calculations are performed. The results of these calculations are in reasonable agreement with available experimental data. The structure of the gas–droplet jet in a cocurrent high-velocity high-temperature gas flow is studied by numerical methods. The ratio of intensities of heat and mass transfer between the phases and turbulent diffusion transfers of substances is found to be different at the initial, transitional, and basic segments of the jet. This difference is responsible for the nonmonotonic axial distribution of vapor density and the lines of the halved mass flow of the condensed phase.

Key words: *gas–droplet turbulent jet, cocurrent flow, numerical simulation.*

Introduction. Injection into a supersonic gas flow was intensely studied in solving today's engineering problems (generation of controlled forces on surfaces in a supersonic flow with injection of liquid and gas side jets [1–3], organization of supersonic combustion above the surface in a supersonic flow, increasing the lift force, or creating an additional drag force [4], jet cooling of surfaces [5–7], etc.).

The main role in studying the interaction of injected jets with the free stream in [1–7] is given to experimental methods. Theoretical research usually involves the use of simplified mathematical models, which allows available solutions to be used in the analysis of similar flows (jet penetration into a motionless medium, flow around solid obstacles, distribution of the explosion waves, etc.).

In earlier research, direct interaction of the disperse phase and the gas was neglected. Appropriate assumptions were first justified in [8–10], where models were constructed, which take into account two-velocity effects and describe the macroscopic turbulent transport of momentum and energy of the phases. Such models of turbulence of a two-phase medium are based on the condition of conservation of momentum for an isolated mole [9]:

$$v'_{10} - v'_1 = \varkappa v'_2. \tag{1}$$

Here $v'_{10} = l_T\,\partial v_{1x}/\partial y$ is the initial fluctuating velocity of the gas mole, v'_i are the final velocities of motion of the gas mole and entrained particles moving to a distance equal to the turbulent mixing length l_T, and $\varkappa$ is the mass concentration of the admixture.

In accordance with Prandtl's hypothesis about the mixing length, the coefficients of turbulent viscosity of the phases are proportional to the velocities of motion of the gas mole and particles entrained by the gas mole [11]:

$$\nu_{T_1} \sim |v'_1| l_T, \qquad \nu_{T_2} \sim |v'_2| l_T.$$

Following [10, 11], we calculated a two-phase turbulent submerged isobaric jet within the framework of the above-mentioned notions. A comparison of the calculated and experimental data shows that they are in good

Mozhaiskii Academy of Military and Space Engineering, St. Petersburg 197082; d_sadin@mail.ru. Translated from Prikladnaya Mekhanika i Tekhnicheskaya Fizika, Vol. 49, No. 3, pp. 85–94, May–June, 2008. Original article submitted October 24, 2006; revision submitted June 22, 2007.

agreement if the mixture contains small amounts of fine particles. As the characteristic diameter of particles and their mass fraction increase, the difference in results becomes more pronounced, which implies that an essential physical factor is neglected. A refined model of interaction of the gas mole and the group of particles entrained by this gas mole is described below.

The processes of heat and mass transfer between the phases also play an important role in modeling the interaction of gas–droplet jets with high-temperature gas flow. Models of turbulence were constructed, and processes of hydrodynamics and heat and mass transfer in a two-phase gas–vapor–droplet flow in a tube (see [12] and the references therein). In the case of intense heat and mass transfer, the equations for the changes in the droplet radius and momentum of the condensed phase have to take into account the correlations $\langle \rho_2' v_{2y}' \rangle$ between the fluctuations of the particle density and the transverse velocity of the particles; the equation of momentum of the gas phase should involve the correlations $\langle \rho_{1v}' v_{1y}' \rangle$ between the fluctuations of the vapor density and the transverse velocity of the gas.

Formulation of the Problem. We consider a two-phase disperse mixture of droplets with a two-species carrier phase (inert gas and vapor) under the known assumptions [13]. In addition, we make allowance for turbulent viscosity, thermal conductivity, and diffusion of the phases in the direction perpendicular to the prevailing flow direction (the x axis coincides with the main flow direction and the y axis coincides with the radial flow direction).

Presenting all parameters as a sum of the mean and fluctuating components, we perform the standard averaging procedure. We also assume that turbulent transport effects prevail over molecular transport effects. If triple correlations are neglected, the equations of turbulent motion of the mixture of the two-species gas and droplets acquire the form

$$\frac{\partial \rho_{1g}}{\partial t} + \nabla \cdot (\rho_{1g} \boldsymbol{v}_1) = 0,$$

$$\frac{\partial \rho_{1v}}{\partial t} + \nabla \cdot (\rho_{1v} \boldsymbol{v}_1) = -J_{12} - \frac{1}{y^\nu} \frac{\partial y^\nu \langle \rho_{1v}' v_{1y}' \rangle}{\partial y},$$

$$\frac{\partial \rho_2}{\partial t} + \nabla \cdot (\rho_2 \boldsymbol{v}_2) = J_{12} - \frac{1}{y^\nu} \frac{\partial y^\nu \langle \rho_2' v_{2y}' \rangle}{\partial y},$$

$$\frac{\partial \rho_2 r}{\partial t} + \nabla \cdot (\rho_2 r \boldsymbol{v}_2) = \frac{4}{3} r J_{12} - \frac{1}{y^\nu} \frac{\partial y^\nu r \langle \rho_2' v_{2y}' \rangle}{\partial y},$$

$$\frac{\partial \rho_1 \boldsymbol{v}_1}{\partial t} + \nabla(\rho_1 \boldsymbol{v}_1 \boldsymbol{v}_1) = -\alpha_1 \nabla p - \frac{1}{y^\nu} \frac{\partial y^\nu \rho_1 \langle v_{1x}' v_{1y}' \rangle}{\partial y} \boldsymbol{i} - \frac{1}{y^\nu} \frac{\partial y^\nu v_{1x} \langle \rho_{1v}' v_{1y}' \rangle}{\partial y} \boldsymbol{i} + \alpha_1 J_{12} \boldsymbol{w}_{12} - J_{12} \boldsymbol{v}_1 - \alpha_1 \boldsymbol{F}_\mu, \quad (2)$$

$$\frac{\partial \rho_2 \boldsymbol{v}_2}{\partial t} + \nabla(\rho_2 \boldsymbol{v}_2 \boldsymbol{v}_2) = -\alpha_2 \nabla p - \frac{1}{y^\nu} \frac{\partial y^\nu \rho_2 \langle v_{2x}' v_{2y}' \rangle}{\partial y} \boldsymbol{i} - \frac{1}{y^\nu} \frac{\partial y^\nu v_{2x} \langle \rho_{2v}' v_{2y}' \rangle}{\partial y} \boldsymbol{i} + \alpha_2 J_{12} \boldsymbol{w}_{12} + J_{12} \boldsymbol{v}_2 + \alpha_1 \boldsymbol{F}_\mu,$$

$$\frac{\partial \rho_2 u_2}{\partial t} + \nabla \cdot (\rho_2 u_2 \boldsymbol{v}_2) = Q_{\Sigma 2} + J_{12} u_{2\Sigma} - \frac{1}{y^\nu} \frac{\partial y^\nu \rho_2 c_2 \langle T_2' v_{2y}' \rangle}{\partial y} - \rho_2 \langle v_{2x}' v_{2y}' \rangle \frac{\partial v_{2x}}{\partial y},$$

$$\frac{\partial}{\partial t} (\rho_1 E_1 + \rho_2 E_2) + \nabla \cdot (\rho_1 E_1 \boldsymbol{v}_1 + \rho_2 E_2 \boldsymbol{v}_2) + \nabla \cdot (p(\alpha_1 \boldsymbol{v}_1 + \alpha_2 \boldsymbol{v}_2))$$

$$- \frac{1}{y^\nu} \frac{\partial y^\nu v_{1x} \rho_1 \langle v_{1x}' v_{1y}' \rangle}{\partial y} - \frac{1}{y^\nu} \frac{\partial y^\nu v_{2x} \rho_2 \langle v_{2x}' v_{2y}' \rangle}{\partial y} - \frac{1}{y^\nu} \frac{\partial y^\nu \rho_1 c_{p1} \langle T_1' v_{1y}' \rangle}{\partial y} - \frac{1}{y^\nu} \frac{\partial y^\nu \rho_2 c_2 \langle T_2' v_{2y}' \rangle}{\partial y}.$$

Here the subscripts g and v refer to the parameters of the inert and vapor species of the gas, respectively, and the subscript Σ refers to the parameters of the surface phase (Σ-phase), the fluctuating components of the parameters are primed; ρ_i, $\boldsymbol{v}_i$, and α_i are the densities, velocity vectors, and volume fractions of the ith phase, r is the droplet radius, E_i, u_i, and T_i are the specific total and internal energies and temperatures of the ith phase, p is the gas pressure, $\boldsymbol{F}_\mu$, J_{12}, and $Q_{\Sigma 2}$ are the intensities of viscous force interaction between the phases, phase transfer, and heat transfer, t is the time, and $\boldsymbol{i}$ is the unit vector in the x direction; the superscripts $\nu = 0$ and 1 refer to the plane and cylindrical coordinate systems.

Closing Relations. The heat and mass transfer between the phases is calculated within the framework of the equilibrium model of the interface (the mean temperature on the droplet surface equals the saturation temperature $T_\Sigma = T_s$) [13]:

$$J_{12} l(p_v) = Q_{\Sigma 1} + Q_{\Sigma 2}, \qquad Q_{\Sigma i} = 3\alpha_2 \,\mathrm{Nu}_i \,\lambda_i (T_s - T_i)/(2r^2).$$

Here $l(p_v)$ is the heat of vapor formation, p_v is the partial pressure of the vapor, λ_i and Nu_i are the thermal conductivity and the Nusselt number of the ith phase ($\mathrm{Nu}_2 = 10$ [13] and Nu_1 is found from the experiment [14]).

The system of conservation equations (2) is closed by the equations of state of calorically perfect gas species

$$p_g = \rho^0_{1g} R_{1g} T_1, \qquad p_v = \rho^0_{1v} R_{1v} T_1, \qquad p = p_g + p_v,$$

$$\rho^0_1 = \rho^0_{1g} + \rho^0_{1v}, \qquad k_{1g} = \rho^0_{1g}/\rho^0_1, \qquad k_{1v} = \rho^0_{1v}/\rho^0_1 \qquad (k_{1g} + k_{1v} = 1),$$

$$u_1 = k_{1g} u_{1g} + k_{1v} u_{1v}, \qquad \lambda_1 = \lambda_1(k_{1g}, T_1),$$

$$i_g = c_g (T_1 - T^*) + i^*_g, \qquad i_v = c_v (T_1 - T^*) + i^*_v,$$

where p_g, R_{1g}, and R_{1v} are the partial pressure of the inert gas and the constants of the gas species, ρ^0_{1g}, ρ^0_{1v}, k_{1g}, k_{1v}, u_{1g}, and u_{1v} are the true densities, concentrations, and internal energies of the unit masses of the species, c_g and c_v are the thermal conductivities of the inert gas and vapor at constant pressure, the asterisk used as a superscript corresponds to fixed parameters, and i_g is the enthalpy of the gas species. The enthalpy of the vapor species i_v is related to the enthalpy of the condensed phase i_l by the normalization condition [13]

$$i^*_v - i^*_l = l(p^*_v) + (c_l - c_v)(T_s(p^*_v) - T^*),$$

where c_l is the heat capacity of the liquid.

To determine the relation between the correlations of the fluctuating components in Eq. (2) and the mean parameters, we use the Boussinesq relations

$$-\langle v'_{1x} v'_{1y} \rangle = \nu_{T_1} \frac{\partial v_{1x}}{\partial y}, \qquad -\langle v'_{2x} v'_{2y} \rangle = \nu_{T_2} \frac{\partial v_{2x}}{\partial y},$$

$$-\langle \rho'_{1v} v'_{1y} \rangle = \frac{\nu_{T_1}}{\mathrm{Sc}_{T_1}} \frac{\partial \rho_{1v}}{\partial y}, \qquad -\langle \rho'_2 v'_{2y} \rangle = \frac{\nu_{T_2}}{\mathrm{Sc}_{T_2}} \frac{\partial \rho_2}{\partial y},$$

$$-\langle T'_1 v'_{1y} \rangle = \frac{\lambda_{T_1}}{\rho_1 c_p} \frac{\partial T_1}{\partial y}, \qquad -\langle T'_2 v'_{2y} \rangle = \frac{\lambda_{T_2}}{\rho_2 c_2} \frac{\partial T_2}{\partial y},$$

$$\mu_{T_i} = \nu_{T_i} \rho_i, \qquad \lambda_{T_1} = c_p \mu_{T_1}/\mathrm{Pr}_T, \qquad \lambda_{T_2} = c_2 \mu_{T_2}/\mathrm{Pr}_T.$$

Here μ_{T_1}, μ_{T_2} and λ_{T_1}, λ_{T_2} are the turbulent viscosities and thermal conductivities of the phases, respectively, Sc_{T_1} and Sc_{T_2} are the turbulent Schmidt numbers and Pr_T is the Prandtl number, and c_p and c_2 are the specific heats at constant pressure of the gas and droplets, respectively.

To construct the refined model of turbulence of a two-phase medium, we consider a simplified scheme of motion of a turbulent mole. At the moment of its nucleation, the turbulent gas mole has two components of the velocity vector: mean axial velocity v_{1x} and fluctuating velocity v'_{10}. After moving to a distance equal to the turbulent mixing length l_T, the mole is not isolated and populated by the same particles because of the difference in phase velocities. Thus, the greater the slip velocity of the phases in the axial and radial directions ($\boldsymbol{v}'_{12} = \boldsymbol{v}'_1 - \boldsymbol{v}'_2$), the greater the error in the condition of conservation of momentum for an isolated mole. The particular value depends on the time of velocity relaxation of the phases [15]:

$$t^{(v)}_1 = \frac{16}{3} \frac{r}{\alpha_2 |w_0|}, \qquad t^{(v)}_2 = \frac{16}{3} \frac{r}{\alpha_1 |w_0|} \frac{\rho^0_2}{\rho^0_1}, \qquad \mathrm{Re}_{12} > 50,$$

$$t^{(\mu)}_1 = \frac{2}{9} \frac{\rho^0_1 r^2}{\mu_1 \alpha_2}, \qquad t^{(\mu)}_2 = \frac{2}{9} \frac{\rho^0_2 r^2}{\mu_1 \alpha_1}, \qquad \mathrm{Re}_{12} < 1, \tag{3}$$

$$\mathrm{Re}_{12} = 2r\rho^0_1 |\boldsymbol{v}_{12}|/\mu_1, \qquad \boldsymbol{v}_{12} = \boldsymbol{v}_1 - \boldsymbol{v}_2.$$

Here ρ_i^0 are the true densities of the phases, μ_1 is the dynamic viscosity of the gas, and w_0 is the characteristic value of the initial slip velocity of the phases.

As Eq. (3) implies, the greater and heavier the droplets, the greater the velocity of the relative motion of the phases. Thus, the condition of conservation of momentum for the turbulent mole should involve the additional virtual mass of the condensed phase $\varkappa_*$, which depends on the fluctuating velocity v'_{10}, time of relaxation $t_1^{(\mu)}$ ($t_1^{(v)}$) of the gas mole, turbulent mixing length l_T, and characteristic scale of turbulence Λ [1]:

$$\varkappa_*/\varkappa = f(v'_{10}, t_1^{(\mu)}, l_T, \Lambda).$$

It follows from the analysis of dimensions that

$$\varkappa_*/\varkappa = f(\mathrm{Sh}_T, \Lambda/l_T), \qquad \mathrm{Sh}_T = |v'_{10}|t_1^{(\mu)}/l_T \tag{4}$$

(Sh_T is the turbulent Strouchal number).

For axisymmetric jets in a cocurrent flow, the experimentally validated conditions [1]

$$\frac{\Lambda}{b} \approx \mathrm{const}, \qquad \frac{l_T}{b} \approx \mathrm{const}, \qquad \frac{\Lambda}{l_T} = \frac{\Lambda}{b}\,\frac{b}{l_T} \approx \mathrm{const},$$

where b is the width of the shear zone, can be reasonably used in Eq. (4).

To determine the relative fluctuating velocity of the phases $v'_{12} = v'_1 - v'_2$, we use the system of equations with allowance for the virtual mass of the condensed phase:

$$\frac{dv'_1}{dt} = -\frac{1}{t_1^{(\mu)}}\,(v'_1 - v'_2), \qquad \frac{dv'_2}{dt} = \frac{1}{t_2^{(\mu)}}\,(v'_1 - v'_2),$$

$$t_1^{(\mu)} = \frac{2}{9}\,\frac{\rho_1 r^2}{\mu_1\alpha_1\alpha_2}, \qquad t_2^{(\mu)} = \frac{2}{9}\,\frac{\rho_1\varkappa_* r^2}{\mu_1\alpha_1\alpha_2}.$$

After replacing the variables

$$V = \rho_1(v'_1 + \varkappa_* v'_2), \quad W = v'_1 - v'_2 = \frac{\rho_* v'_1 - V}{\rho_1\varkappa_*} = \frac{V - \rho_* v'_2}{\rho_1}, \quad \rho_* = \rho_1(1 + \varkappa_*),$$

we obtain the system

$$\frac{dV}{dt} = 0, \qquad \frac{dW}{dt} = -\lambda W, \qquad \lambda = \frac{1}{t_1^{(\mu)}} + \frac{1}{t_2^{(\mu)}}$$

and its solution $V = V_0$, $W = W_0\,\mathrm{e}^{-\lambda t}$. Returning to the original variables, we obtain

$$v'_i = v'_{i0}\,\mathrm{e}^{-\lambda t} + \rho_1(v'_1 + \varkappa_* v'_2)(1 - \mathrm{e}^{-\lambda t})/\rho_*. \tag{5}$$

For final determination of the relative fluctuating velocity of the phases resulting from mole displacement to a distance equal to the mixing length l_T, with allowance for the virtual mass, we integrate Eq. (5). Finally, we obtain

$$l_T = \frac{v'_{20}}{\lambda}\,(1 - \mathrm{e}^{-\lambda T}) + \frac{\rho_1(v'_1 + \varkappa_* v'_2)}{\rho_*}\Big(t + \frac{1}{\lambda}\,\mathrm{e}^{-\lambda T} - \frac{1}{\lambda}\Big). \tag{6}$$

Equation (6) determines the time T of mole motion before it s merging with the next layer. With allowance for that, we use Eq. (5) to find the relative fluctuating velocity of the phases with the initial conditions $v'_{10} = l_T\,\partial v_{1x}/\partial y$ and $v'_{20} = 0$:

$$v'_{12}/v'_{10} = \mathrm{e}^{-\lambda T}\,.$$

Thus, the turbulent viscosities of the phases are described by the equations

$$\mu_{T_1} = \rho_1 l_T^2\,\frac{1 + \varkappa_*\,\mathrm{e}^{-\lambda T}}{1 + \varkappa_*}\,\Big|\frac{\partial v_{1x}}{\partial y}\Big|, \qquad \mu_{T_2} = \rho_2 l_T^2\,\frac{1 - \mathrm{e}^{-\lambda T}}{1 + \varkappa_*}\,\Big|\frac{\partial v_{1x}}{\partial y}\Big|.$$

For final closure of system (2) in accordance with the chosen model, we have to find the mixing length l_T. We use the classical approach [16]

$$\frac{db}{dx} = \frac{c}{2}\,\frac{(v_{1m} - v_{1h})(1 + \rho_h/\rho_m)}{v_{1m} + v_{1h}\rho_h/\rho_m}, \qquad l_T = c_1 b.$$

Here the subscripts m and h correspond to the parameters on the jet centerline and the cocurrent flow centerline; the recommended values of the constants are $c = 0.27$ on the initial segment and $c = 0.22$ on the main segment; $c_1 = 0.1$ [1].

Initial and Boundary Conditions. The initial data imply an undisturbed flow in the entire computational domain. Parameters of injection of a two-phase medium are set in a cylindrical coordinate system on the left boundary at $x = 0$, $0 \leqslant y \leqslant R$ (R is the nozzle radius), the cocurrent flow parameters are set at $R < y \leqslant Y$ (Y is the outer radial boundary), the conditions of symmetry are imposed at $x \geqslant 0$ and $y = 0$, and the cocurrent flow parameters are again set at $y = Y > b$.

In obtaining the steady-state solution by a time-dependent method, we solved an unsteady problem with imposed initial and boundary conditions. The steady-state regime was assumed to be established when the condition [17]

$$\left| \frac{\rho_i^{k+1} - \rho_i^k}{\rho_i^k \tau} \right| \leqslant \varepsilon$$

was satisfied in all cells of the computational domain. Here τ is the iteration parameter (time step), k is the iteration number, and $\varepsilon = 10^{-3}$–10^{-4}.

A method with splitting with respect to physical processes was developed for the calculations. At the first stage, we calculated only the viscous terms of system (2) by the second-order sweep method. A scheme with allowance for stiffness of the initial equations was used at the second stage [18]. The calculations were performed by a time-dependent method.

Methodical Calculations. To estimate the adequacy of the mathematical model and calculation technique, as well as the degree of influence of terms that describe turbulent transport, we performed a number of methodical calculations.

The calculated and experimental [8] data for two-phase jets are plotted in Figs. 1 and 2. Figure 1 shows the distribution of the relative axial velocity of the gas in the x axis dimension, and the lines of the halved velocity and halved specific mass flow of particles are shown in Fig. 2 (d [μm] is the particle diameter, $\varkappa_0$ is the mass concentration of particles, and v_{1m0} is the axial velocity of the gas on the nozzle exit at $x = 0$).

The function that takes into account the virtual mass of the condensed phase was chosen on the basis of experimental data [8] in the approximation of the linear dependence of the virtual mass on the turbulent Strouchal number in the form $\varkappa_*/\varkappa = 2\,\mathrm{Sh}_T + 1$ and was calculated at each point of the computational domain. In defining the form of the functional dependence, we took into account that $t_1^{(\mu)} \to 0$, $\mathrm{Sh}_T \to 0$, and $\varkappa_* \to \varkappa$ for small relaxation times. The calculated results are in reasonable agreement with experimental data. The discrepancy in these data in the region close to the nozzle (see Fig. 2) can be explained by the nonuniform initial profile of velocities in the nozzle [8]. The dashed curve $4'$ in Fig. 1 shows the calculation with ignored virtual mass of particles with $d = 32$ μm and $\varkappa_0 = 1.4$ for the case where the particle concentration is commensurable in terms of density with the carrier phase. The difference between the calculated axial velocity and experimental data is approximately 40%, which testifies that slipping of the phases exerts a significant effect in the case of turbulent fluctuations.

The convergence of the method was tested on gradually refined computational grids and with a decreasing time step. In addition, we analyzed the data calculated for a turbulent subsonic gas–droplet jet in a cocurrent gas flow with $\theta = 1/3$, $m = v_h/v_{m0} = 5$, $\varkappa_0 = 1$, and $r_0 = 25$ μm without allowance for the correlation $\langle \rho'_{1v} v'_{1y} \rangle$ between the fluctuations of vapor density and transverse velocity of the gas and also without allowance for the correlation $\langle \rho'_2 v'_{2y} \rangle$ between the fluctuations of particle density and transverse velocity of particles. A significant discrepancy between these results and the data obtained by model (2) suggests that these factor exert a substantial effect in the case of a nonisothermal gas–droplet jet with intense heat and mass transfer.

Calculation Results. A gas–droplet jet in the state of phase equilibrium in the isobaric mode $n = 1$ is injected in the axial direction x into an infinite homogeneous flow of a calorically perfect viscous gas. The calculations were performed for the following values of the gas parameters: gas constant $R_1 = 320$ J/(kg·K), ratio of specific heats $\gamma = 1.2$, and Mach numbers $\mathrm{M}_h = 0.66$ and 1.33. The following injection parameters were used: relative velocity $m = v_{1h}/v_{10} = v_{1h}/v_{20} = 5$ and 10, nonisothermality $\theta = 0.2$ and ratio of stagnation temperatures $\theta^* = 0.172$, respectively, for subsonic and supersonic cocurrent flows, droplet radius at the nozzle exit $r_0 = 25$ μm, the properties of water droplets and vapor were taken from the tables [19] and approximated by fifth-order polynomials, and the initial mass concentration of the condensed phase $\varkappa_0$ was varied from 0.1 to 5.

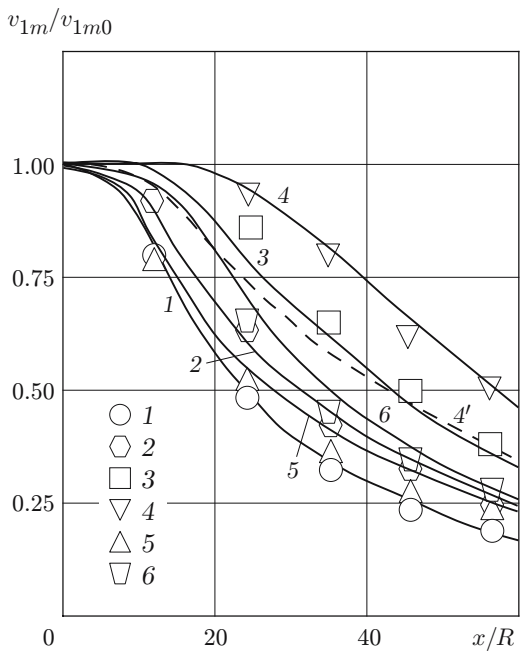

Fig. 1

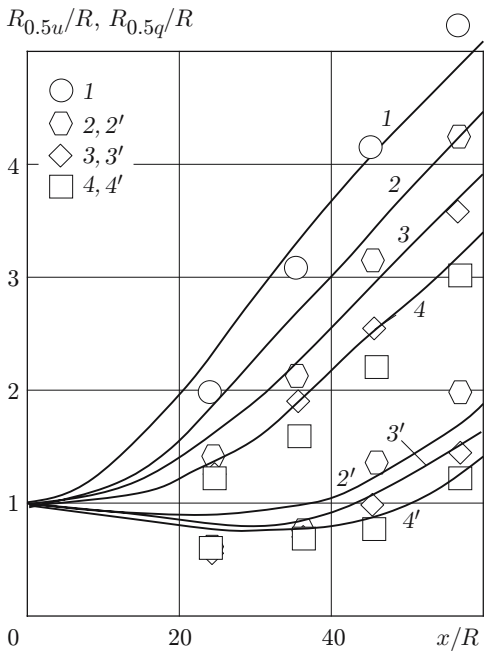

Fig. 2

Fig. 1. Distribution of the relative axial velocity of the gas on the x axis: 1) the curves and points refer to a one-phase jet; 2) $d = 32$ μm and $\varkappa_0 = 0.3$; 3) $d = 32$ μm and $\varkappa_0 = 0.77$; 4) $d = 32$ μm and $\varkappa_0 = 1.4$ (curve 4′ shows the data calculated with ignored virtual mass of particles); 5) $d = 72$ μm and $\varkappa_0 = 0.3$; 6) $d = 17$ μm and $\varkappa_0 = 0.56$.

Fig. 2. Lines of the halved velocity (1–4) and halved mass flow of particles (2′–4′): the curves 1 and points 1 refer to a one-phase jet, 2 and 2′ to $d = 32$ μm and $\varkappa_0 = 0.3$, 3 and 3′ to $d = 32$ μm and $\varkappa_0 = 0.56$, and 4 and 4′ to $d = 32$ μm and $\varkappa_0 = 0.77$.

We studied the interaction of a two-phase jet with a subsonic ($M_h = 0.66$) cocurrent gas flow. Figure 3 shows the fields of the dimensionless gas temperature T_1/T_{m0} and the dimensionless vapor density ρ_{1v}/ρ_{v0} (ρ_{v0} is the equilibrium value of the vapor density of the injected two-phase medium) for $\varkappa_0 = 1$.

The two-phase jet has an initial cone-shaped region $0 \leqslant x \leqslant x_t$ (x_t is the abscissa of the transitional cross section) with gasthermodynamic parameters of the phases at the nozzle exit. Outside this initial region, there occurs viscous turbulent nonequilibrium interaction of the gas–droplet jet and the external cocurrent gas flow with intense evaporation of droplets and formation of vapor. Beginning from the abscissa of the transitional cross section x_t, the gas temperature on the axis of symmetry monotonically increases (Fig. 3a). In contrast to the temperature profile, the axial profile of vapor density has a maximum (Fig. 3b), which is explained by different ratios of intensities of vapor formation and turbulent diffusion of the vapor component. The intensity of the phase transition is higher than the intensity of diffusion transport of vapor in the initial region; the opposite situation is observed in the main part of the jet.

Figure 4 shows the lines of the halved mass flow of droplets (m is the relative velocity). An analysis of the results obtained shows that, depending on the parameters $\varkappa_0$ and m, the lines of the halved mass flow can have a nonmonotonic form with two extreme points, the minimum corresponding to the abscissa of the transitional cross section x_t, and the maximum corresponding to the maximum of the axial profile of vapor density.

Figure 5 shows the behavior of the droplet radius on the axis of symmetry for different values of the mass concentration of the condensed phase. At $\varkappa_0 = 0.1$ (curve 1), the droplets become completely evaporated at a distance $x/R > 20$. As the mass fraction of the droplets increases, the droplet radius is almost halved at $\varkappa_0 = 1$ and decreases by less than 20% at $\varkappa_0 = 5$.

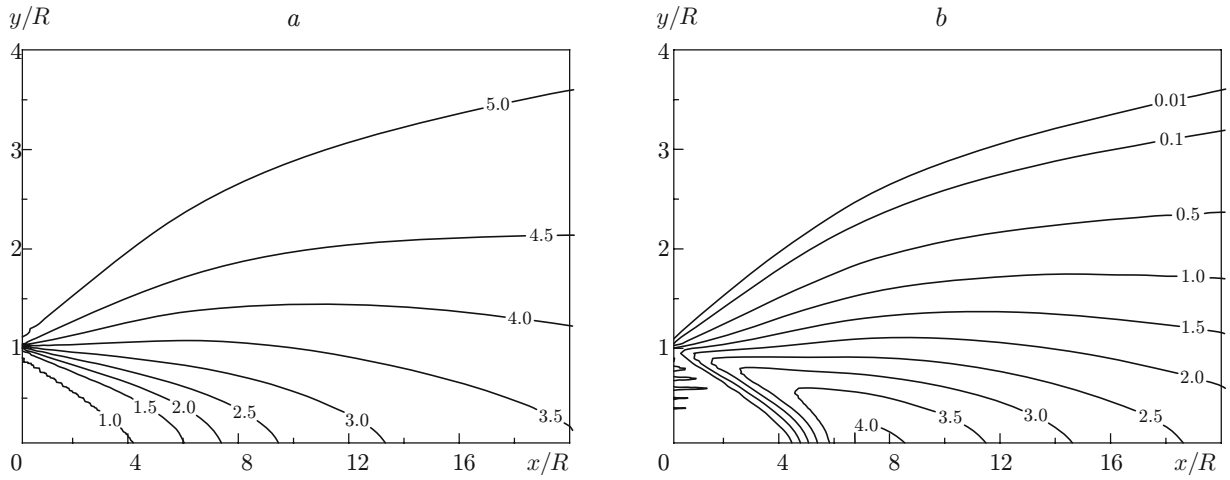

Fig. 3. Fields of the relative gas temperature (a) and vapor density (b) for $\varkappa_0 = 1$.

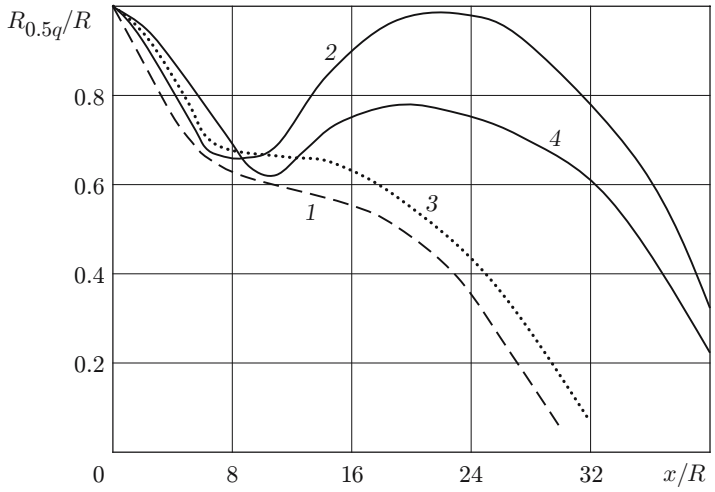

Fig. 4. Lines of the halved mass flow of droplets: 1) $m = 10$ and $\varkappa_0 = 1$; 2) $m = 10$ and $\varkappa_0 = 5$; 3) $m = 5$ and $\varkappa_0 = 0.2$; 4) $m = 5$ and $\varkappa_0 = 1$.

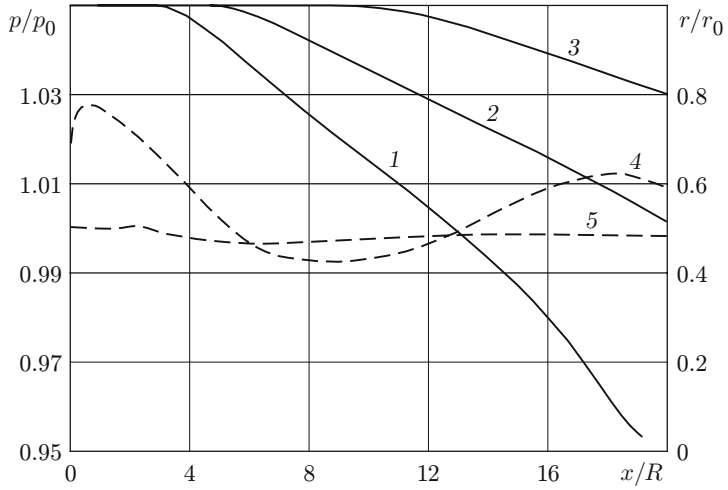

Fig. 5. Droplet radius (1–3) and pressure (4 and 5) on the axis of symmetry for $m = 10$ and $\varkappa_0 = 0.1$ (1), 1 (2), and 5 (3); curves 4 and 5 refer to $M_h = 1.33$ and 0.66, respectively.

Injection of a two-phase jet into a supersonic ($M_h = 1.33$) cocurrent gas flow has a special feature: in such an interaction, the gas is decelerated to a subsonic velocity through a shock wave (curve 4 in Fig. 5), in contrast to an almost isobaric subsonic ($M_h = 0.66$) flow (curve 5). The gas pressure distributions along the axis of symmetry (curves 4 and 5) were calculated for supersonic and subsonic cocurrent flows with $\varkappa_0 = 1$ and $m = 10$.

This work was supported by the Russian Foundation for Basic Research (Grant No. 05-08-50120a).

REFERENCES

1. J. Schetz, *Injection and Mixing in Turbulent Flow*, Inst. of Aeronaut. and Astronaut., New York (1980).
2. N. D. Kovalenko, *Disturbances in a Supersonic Flow due to Mass and Heat Supply* [in Russian], Naukova Dumka, Kiev (1980).
3. A. M. Teverovskii, "Investigation of the physical pattern of interaction of the size jet with a supersonic flow," CIAM Paper No. 487, Moscow (1971).
4. *Gas Flow with Heat Supply near the External Surface of the Body: Foreign Scientific Publications in 1949–1970* [Russian translation], Moscow (1971).
5. V. P. Isachenko and V. I. Kushnyrev, *Jet Cooling* [in Russian], Énergoatomizdat, Moscow (1984).
6. K. Yanagi, "Cooling of a high-temperature surface by liquid droplets," *Nenre Kekai Si*, **55**, No. 595, 892–897 (1976).
7. R. Z. Alimov, "Heat transfer in a two-phase flow around a transversely located heated cylindrical tube," *Zh. Teor. Fiz.*, **26**, No. 6, 1292–1305 (1956).
8. M. K. Laats and F. A. Frishman, "Assumptions used for two-phase jet calculations," *Izv. Akad. Nauk SSSR, Mekh. Zhidk. Gaza*, No. 2, 186–191 (1970).
9. G. N. Abramovich, "Effect of the admixture of solid particles or droplets on the structure of a turbulent gas jet," *Dokl. Akad. Nauk SSSR*, **190**, No. 5, 1052–1055 (1970).
10. G. N. Abramovich, V. I. Bazhanov, and T. A. Girshovich, "Turbulent jet with heavy admixtures," *Izv. Akad. Nauk SSSR, Mekh. Zhidk. Gaza*, No. 6, 41–49 (1972).
11. A. P. Vasil'kov, "Calculation of a two-phase turbulent isobaric jet," *Izv. Akad. Nauk SSSR, Mekh. Zhidk. Gaza*, No. 5, 57–63 (1976).
12. V. I. Terekhov and M. A. Pakhomov, "Numerical study of the near-wall gas–droplet jet in a tube with a heat flux on the surface," *J. Appl. Mech. Tech. Phys.*, **47**, No. 1, 1–11 (2006).
13. R. I. Nigmatulin, *Dynamics of Multiphase Media*, Part 1, Hemisphere Publ., New York (1991).
14. A. F. Chudnovskii, *Heat Transfer in Disperse Media* [in Russian], Gostekhteorizdat, Moscow (1954).
15. D. V. Sadin, "Stiffness of systems with partial derivatives that describe motion of heterogeneous media," *Mat. Model.*, **14**, No. 11, 43–53 (2002).
16. G. N. Abramovich, *Applied Gas Dynamics* [in Russian], Nauka, Moscow (1976).
17. V. M. Kovenya and N. N. Yanenko, *Splitting Method in Gas-Dynamic Problems* [in Russian], Nauka, Novosibirsk (1981).
18. D. V. Sadin, "Stiffness problem in modeling wave flows of heterogeneous media with a three-temperature scheme of interphase heat and mass transfer," *J. Appl. Mech. Tech. Phys.*, **43**, No. 2, 286–290 (2002).
19. P. L. Kirillov, Yu. S. Yur'ev, and V. P. Bobkov, *Handbook on Thermal and Hydraulic Design* (*Nuclear Reactors, Heat Exchangers, and Steam Generators*) [in Russian], Énergoatomizdat, Moscow (1990).